

Reviewing the Antioquia batholith and satellite bodies: a record of Late Cretaceous to Eocene syn- to post-collisional arc magmatism in the Central Cordillera of Colombia

*José Duque-Trujillo¹, Camilo Bustamante¹, Luigi Solari², Álvaro Gómez-Mafla¹,
Gloria Toro-Villegas¹, Susana Hoyos¹

¹ Departamento de Ciencias de la Tierra, Universidad EAFIT, Carrera 49 No. 7 sur-50, Medellín, Colombia.

jduquestr@eafit.edu.co, cbustam3@eafit.edu.co, agomez@eafit.edu.co, gtoro@eafit.edu.co, shoyosm1@eafit.edu.co

² Universidad Nacional Autónoma de México, Centro de Geociencias, Campus Juriquilla, Blvd. Juriquilla No. 3001, 76230, Querétaro, México.
solari@unam.mx

* Corresponding author: jduquestr@eafit.edu.co

ABSTRACT. The Antioquia batholith represents the magmatic record of the interaction between the Farallón and Caribbean plates with the NW part of the South American Plate during the Meso-Cenozoic. Several authors have reported zircon U-Pb ages and whole rock geochemistry in order to constrain the crystallization history of this batholith and its formation conditions. The present work aims to gather the existing data with new data obtained from the Ovejas batholith and La Unión stock, both genetically related to the main intrusion. Gathering our new data with information obtained in previous works, we conclude that the Antioquia batholith was constructed by successive pulses from *ca.* 97 to 58 Ma in an arc-related setting. The initial pulses are related to syn-collisional tectonics, during the early interaction between the Farallón plate and NW South America. The final pulses, that record Eocene ages, are related to a post-collisional setting, similar to that recorded in other plutons of the Paleogene magmatic arc of the Central Cordillera.

Keywords: Antioquia Batholith, Magmatism, Central Cordillera, Colombia.

RESUMEN. Revisión sobre el Batolito Antioqueño y sus cuerpos satélites: registro del magmatismo syn- a poscolisional entre el Cretácico tardío y Eoceno en la cordillera Central de Colombia. El Batolito Antioqueño representa el registro magmático de la interacción entre las placas Farallón y Caribe con la parte NW de la placa Sudamericana durante el Meso-Cenozoico. Varios autores han obtenido edades U-Pb en circon y geoquímica de roca total con el objetivo de definir el ambiente de formación y la historia magmática de este importante cuerpo intrusivo. El presente trabajo pretende reunir los datos hasta ahora existentes junto con nuevos datos sobre los cuerpos satélites de Ovejas y La Unión, ambos relacionados genéticamente con la masa principal del batolito. De esta compilación, concluimos que el Batolito Antioqueño fue formado por una serie de pulsos magmáticos entre ~97 y 58 Ma en un ambiente de arco magmático. Las fases iniciales de este magmatismo corresponden a un ambiente tectónico syn-colisional correspondiente a las fases iniciales de la interacción entre las placas Farallón y NW de la placa Sudamericana. Mientras que las fases finales, de edad eoceno, se relacionan con un ambiente poscolisional, similar al registrado en otros plutones del arco magmático Paleógeno de la cordillera Central en Colombia.

Palabras clave: Batolito Antioqueño, magmatismo, Cordillera central, Colombia.

I. Introduction

Granite batholiths are found in continental magmatic arcs around the world and constitute the main vestiges of subduction-related settings (Best, 2013). These are constructed over time spans from 10^5 to 10^6 years by the incremental assembly of small magma batches (Coleman *et al.*, 2004; Annen *et al.*, 2015).

In that sense, they can record significant changes in the tectonic style of convergent margins through time, identified when U-Pb geochronology in zircons and whole rock geochemistry is combined and its spatial distribution is considered. The whole Andean chain includes several Meso-Cenozoic granitoids that record the continuous subduction setting that has molded the western margin of South America since the breakup of Pangea during the Triassic (Ramos, 2009; Ramos and Aleman, 2000). Hence, studying these granitoids may help to unravel evolution of the continental margin.

A major arc-continent collisional event took place in the western margin of northern South America related to its interaction with the Caribbean Large Igneous Province during Late Cretaceous (Cardona *et al.*, 2011; Villagómez *et al.*, 2011; Bayona *et al.*, 2012; Spikings *et al.*, 2015; Jaramillo *et al.*, 2017). A contemporaneous granitic magmatism appeared in the Central Cordillera represented by the intrusion of the Antioquia batholith, a granodiorite to tonalite pluton formed by multiple pulses from *ca.* 90 to 60 Ma (Ibáñez-Mejía *et al.*, 2007; Restrepo-Moreno *et al.*, 2009; Ordóñez and Pimentel, 2001; Ordóñez-Carmona *et al.*, 2006; Leal-Mejía, 2011; Villagómez *et al.*, 2011). This was succeeded by a Paleogene post-collisional magmatic arc which includes the Eocene portion of the Antioquia batholith (Leal-Mejía, 2011; Bayona *et al.*, 2012; Bustamante *et al.*, 2017). The latter suggests that the continental margin was subjected to a progressive thickening since its interaction with the Farallón plate, and that may be recorded by the Antioquia batholith.

However, geochemical and geochronological data from this batholith are limited to scarce international works presenting extensive formation ages and discussing the origin of the Antioquia Batholith in a long term tectonic model including both the transition from Nazca-dominated to Caribbean-dominated tectonics.

In this paper, we present new U-Pb crystallization ages from one of the earliest (La Unión stock) and intermediate (Ovejas batholith) pulses of the Antioquia batholith, and also provide new whole rock geochemistry. This information combined with a compilation of available data obtained from previous works, will allow us to outline the crystallization history of the Antioquia batholith in relation with the Meso-Cenozoic subduction setting of the NW corner of the South American Plate, tracking the thickening that experienced the margin during the Late Cretaceous and lasted until the Eocene.

2. Geological setting

Three N-NE trending Cordilleras built the Andes of Colombia. The Eastern Cordillera, mainly constituted by a Proterozoic metamorphic basement covered by highly deformed Paleozoic to Cenozoic sedimentary sequences (Villamil, 1999; Sarmiento-Rojas *et al.*, 2006). This cordillera is separated from the Central Cordillera by the Magdalena River Valley, which in turn consists of Permo-Triassic gneisses, migmatites and amphibolites (Martens *et al.*, 2014) and Jurassic schists belts (Blanco-Quintero *et al.*, 2014; Bustamante *et al.*, 2017) intruded by Jurassic (Cochrane *et al.*, 2014; Bustamante *et al.*, 2016) and Cretaceous to Paleogene arc-related plutons respectively (Bayona *et al.*, 2012; Bustamante *et al.*, 2017). The northernmost exposure of the latter magmatic belt continues under the Lower Magdalena Valley, represented by the Bonga pluton (Mora-Bohórquez *et al.*, 2017). The Cauca River Valley separates the Central Cordillera from the Western Cordillera which includes Late Cretaceous oceanic rocks accreted to the South American plate during Early Cretaceous (Kerr *et al.*, 1997; Villagómez and Spikings, 2013), then intruded by Miocene plutons and covered volcanic rocks from intermediate to tholeiitic character (Bissig *et al.*, 2017; Restrepo and Toussaint, 1990).

2.1. Late Cretaceous to Paleogene magmatism of the Colombian Andes

Late Cretaceous arc-related granitoids (*i.e.*, Antioquia batholith) intrudes the Great Caribbean Arc (Fig. 1). These have been identified all along the Central Cordillera of Colombia (Ibáñez *et al.*, 2007; Villagómez *et al.*, 2011; Restrepo-Moreno, *et al.*, 2009; Leal-Mejía, 2011) as well as in the Real

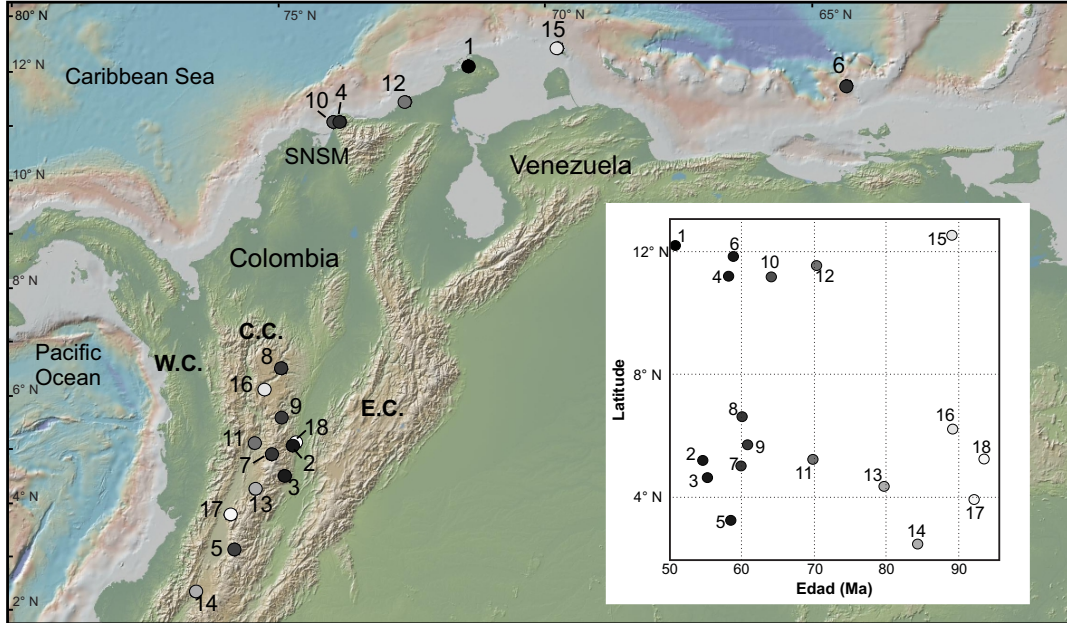


FIG. 1. Geographic distribution of the Late Cretaceous to Paleogene magmatism in the northwestern part of the South American Plate.

1. Parashi Pluton; 2. El Hatillo Stock; 3. El Bosque Batholith; 4. Santa Marta Batholith; 5. Santa Bárbara Batholith; 6. La Blanquilla Pluton; 7. Manizales Stock; 8. Antioquia Batholith; 9. Sonson Batholith; 10. Playa Salguero Stock; 11. Irra Stock; 12. Baja Guajira Granitoid; 13. Córdoba Stock; 14. Jejenes Stock; 15. Aruba Batholith; 16. Media Luna Stock; 17. Buga Batholith; 18. Mariquita Stock. Abbreviation: W.C.: Western Cordillera; C.C.: Central Cordillera; E.C.: Eastern Cordillera.

Cordillera in Ecuador (Vallejo *et al.*, 2009). These are the main vestiges of a well established subduction zone on the western margin of South America that lasted until at least the middle Eocene (Fig. 1), when magmatism stopped due to difficulties of the Caribbean plateau to subduct and the northward migration of the Caribbean and South America plates (Aspden *et al.*, 1987; Pindell *et al.*, 2005; Spikings *et al.*, 2005; Vallejo *et al.*, 2009; Cardona *et al.*, 2010; Villagómez *et al.*, 2011; Bayona *et al.*, 2012).

2.1.1. Antioquia batholith and related stocks

The Antioquia batholith is the only Late-Cretaceous intrusive body recognized in the Central Cordillera of Colombia and constitutes the first record of the continental arc magmatism in NW South America after *ca.* 20 m.y. of magmatic quiescence (Bustamante *et al.*, 2016).

Along decades, different geochronometers as U-Pb, $^{40}\text{Ar}/^{39}\text{Ar}$, K-Ar, U-Th/He, Fission tracks, Re/Os and Rb/Sr have been used on the Antioquia Batholith, obtaining a considerable dataset. A review of all available geochronological ages are listed in

table 1, where basic data are gathered including sampling site, method, material, error, among others.

In order to establish the formation age of the batholith, extensive U-Pb geochronological studies in zircon, using different techniques (LA-ICP-MS, TIMS and SHRIMP) have been performed (Fig. 2; Table 1). U-Pb have yielded crystallization ages between 97 and 58 Ma (Fig. 3; Ordóñez-Carmona *et al.*, 2006; Correa *et al.*, 2006; Restrepo-Moreno *et al.*, 2007; Ibáñez-Mejía *et al.*, 2007; Leal-Mejía, 2011; Villagómez *et al.*, 2011). The whole intrusive complex has a scanty compositional variation, ranging from granodiorite to tonalite with minor gabbroic facies (Feininger and Botero, 1982). Five spatially related satellite stocks have also been related to this major Cretaceous magmatic body. These satellite stocks are known as the Altavista, La Culebra, Ovejas, La Unión and San Diego. Their compositions range from granite to granodiorite, except the San Diego stock which has a gabbroic composition (Fig. 3A). Based on extensive zircon U-Pb data, Leal-Mejía (2011) defined four main pulses which constructed the Antioquia batholith (i) An older pulse between

TABLE 1. REVIEW OF GEOCHRONOLOGICAL DATA FROM THE ANTIOQUIA BATHOLITH AND SATELLITE BODIES. SAMPLE LOCATIONS ARE PLOTTED IN FIGURE 2.

FID	Sample code	Latitude*	Longitude*	Geological Unit	Rock type	Age (Ma)	Error (\pm Ma)	Method	Material	Reference
66	R6834	6.499	74.753	CS	Quartzdiorite	60.1	1.2	U-Pb (LA)	Zircon	5
42	1	6.418	75.426	AB	Granodiorite	60	-	Rb-Sr	Biotite	3
35	2	6.497	75.388	AB	Granodiorite	58	-	Rb-Sr	Biotite	3
19	4	6.948	75.422	AB	Granodiorite	68	-	Rb-Sr	Biotite	3
10	12038453	5.953	75.355	US	Quartzdiorite	73.5	1.3	U-Pb (LA)	Zircon	17
10	12038453	5.953	75.355	US	Quartzdiorite	82.8	1.5	U-Pb (LA)	Zircon	17
34	1302A	6.497	75.413	AB	Quartzdiorite	79	3	K-Ar	Biotite	1
14	AC75	6.227	75.638	AS	Diorite	96	0.39	U-Pb (LA)	Zircon	16
69	BA12	6.037	74.999	AB	Granodiorite	98	27	Rb-Sr	Whole Rock	6
24	BA2	6.733	75.620	AB	Granodiorite	98	27	Rb-Sr	Whole Rock	6
49	BA32	6.733	75.620	AB	Granodiorite	98	27	Rb-Sr	Whole Rock	6
48	BA4	6.216	75.200	AB	Granodiorite	83	4	Rb-Sr	Whole Rock	7
53	BA6	6.512	75.174	AB	Granodiorite	98	27	Rb-Sr	Whole Rock	6
20	BA7	6.943	75.438	AB	Granodiorite	98	27	Rb-Sr	Whole Rock	6
65	BA9	6.522	74.782	AB	Granodiorite	98	27	Rb-Sr	Whole Rock	6
28	BC1	6.799	75.215	AB	Granodiorite	55.8	2.7	FT	Zircon	11
30	BC2	6.664	75.222	AB	Granodiorite	63.3	3.2	FT	Zircon	11
41	BC3	6.408	75.397	AB	Granodiorite	49.4	2	FT	Zircon	11
18	BC4	6.964	75.434	AB	Granodiorite	62.8	2.9	FT	Zircon	11
33	BC5	6.512	75.410	AB	Monzogranite	60.4	2.3	FT	Zircon	11
31	BC6	6.616	75.154	AB	Granodiorite	58	2.3	FT	Zircon	11
56	BC7	6.536	75.077	AB	Granodiorite	49.1	2.5	FT	Zircon	11
43	BC8	6.204	75.320	AB	Quartzdiorite	53.4	2.7	FT	Zircon	11
68	BC9	6.042	74.999	AB	Quartzdiorite	67.1	2.7	FT	Zircon	11
61	CRI1	6.484	74.923	AB	Dike	61.8	1.3	U-Pb (LA)	Zircon	5
61	CRI1	6.484	74.923	AB	Dike	74.4	1.2	U-Pb (LA)	Zircon	5
76	DV148	6.421	75.385	AB	Granodiorite	55.4	5.2	FT	Zircon	13
55	DV153	6.540	75.122	AB	Granodiorite	69.7	8.6	FT	Apatite	13
77	DV53	6.311	75.505	AB	Diorite	13.4	1.4	U-Th/He	Apatite	14
77	DV53	6.311	75.505	AB	Diorite	72.9	18.8	FT	Apatite	14
78	DV54	6.328	75.481	AB	Diorite	64.1	5.4	Ar/Ar	Hornblende	14
78	DV54	6.328	75.481	AB	Diorite	70.4	6.3	Ar/Ar	Hornblende	14
78	DV54	6.328	75.481	AB	Diorite	74.4	10.6	FT	Apatite	14
78	DV54	6.328	75.481	AB	Diorite	71	1.9	Ar/Ar	Hornblende	14
44	DV56	6.056	75.212	AB	Granite	87.2	1.6	U-Pb (LA)	Zircon	15
75	DV58	6.018	75.135	AB	Granite	32	1.9	U-Th/He	Apatite	14
75	DV58	6.018	75.135	AB	Granite	45.5	3.1	C	Zircon	14
75	DV58	6.018	75.135	AB	Granite	56.5	8.6	Ar/Ar	K Felspar	14
75	DV58	6.018	75.135	AB	Granite	58.5	8	FT	Apatite	14

table 1 continued.

FID	Sample code	Latitude*	Longitude*	Geological Unit	Rock type	Age (Ma)	Error (\pm Ma)	Method	Material	Reference
75	DV58	6.018	75.135	AB	Granite	62.6	1.1	Ar/Ar	K Felspar	14
75	DV58	6.018	75.135	AB	Granite	72.3	0.3	Ar/Ar	Biotite	14
75	DV58	6.018	75.135	AB	Granite	73.2	0.8	Ar/Ar	Biotite	14
75	DV58	6.018	75.135	AB	Granite	31	1.4	U-Th/He	Apatite	14
75	DV58	6.018	75.135	AB	Granite	45.2	1.2	U-Th/He	Zircon	14
75	DV58	6.018	75.135	AB	Granite	63.4	0.5	Ar/Ar	K Felspar	14
75	DV58	6.018	75.135	AB	Granite	71.4	0.2	Ar/Ar	Biotite	14
75	DV58	6.018	75.135	AB	Granite	93.5	1.5	U-Pb (LA)	Zircon	14
70	DV63	5.968	74.959	AB	Granite	74.8	7.4	FT	Zircon	13
72	DV64	5.982	74.955	AB	Granodiorite	63.2	0.3	Ar/Ar	Plagioclase	14
17	DV70	6.971	75.426	AB	Granodiorite	69.1	0.2	Ar/Ar	Biotite	14
54	El1	6.529	75.123	LV	Mineralization	60	0.3	Re-Os	molybdenite	5
52	ER 1	6.499	75.099	ERP	Porphyry	59.9	0.9	U-Pb (LA)	Zircon	5
62	G1	6.508	74.911	-	Alteration	58.7	0.3	Re-Os	Sericite	5
60	G29	6.508	74.917	-	Tonalite	60.7	1	U-Pb (LA)	Zircon	5
79	G9	6.509	74.910	-	Mineralization	58	2	K-Ar	molybdenite	5
59	GRII1	6.511	74.912	AB	Tonalite	59.2	1.2	U-Pb (LA)	Zircon	5
11	JJ253	5.943	75.312	US	Quartzdiorite	64	4	K-Ar	Biotite	10
58	LF10	6.637	74.846	AB	Granodiorite	79.5	1.3	SHRIMP	Zircon	5
32	M11	6.533	75.392	AB	Granitoid	83.75	0.36	TIMS	Zircon	4
64	no name	6.549	74.751	AB	Granodiorite	68	2	K-Ar	-	2
23	Osos15	6.764	75.488	-	Soil	2.79	0.13	FT	Zircon	12
74	PGA05	5.978	74.953	AB	Granitoid	88.46	0.63	TIMS	Zircon	4
51	Santo Domingo 1	6.449	75.134	-	-	59.1	0.3	Re-Os	molybdenite	5
8	SML1	6.236	75.517	MLS	Granodiorite	89.1	1.3	U-Pb (LA)	Zircon	18
5	SPK0526	6.356	75.588	AB	Quartzdiorite	70	3	K-Ar	Biotite	8
27	SPK0528	6.768	75.279	AB	Granodiorite	74	3	K-Ar	Biotite	8
50	SPK0529	6.270	75.094	AB	Quartzdiorite	71	3	K-Ar	Biotite	8
25	SPK0530	6.692	75.575	AB	Quartzdiorite	72	3	K-Ar	Biotite	8
67	SPK0532	6.042	75.008	AB	Quartzdiorite	80	3	K-Ar	Biotite	8
37	SR11	6.460	75.370	AB	Quartzdiorite	43.4	2.2	U-Th/He	Apatite	9
38	SR15	6.450	75.370	AB	Quartzdiorite	48.9	2.4	U-Th/He	Apatite	9
39	SR19	6.450	75.360	AB	Quartzdiorite	40.7	2	U-Th/He	Apatite	9
36	SR2	6.470	75.380	AB	Quartzdiorite	36.6	1.8	U-Th/He	Apatite	9
2	SR26	6.380	75.590	AB	Quartzdiorite	46.7	2.3	U-Th/He	Apatite	9
3	SR31	6.370	75.590	AB	Quartzdiorite	42.9	2.1	U-Th/He	Apatite	9
1	SR32	6.380	75.600	AB	Quartzdiorite	41.3	2.1	U-Th/He	Apatite	9
82	SR41	6.410	75.410	AB	Quartzdiorite	25.1	1.3	U-Th/He	Apatite	9

table 1 continued.

FID	Sample code	Latitude*	Longitude*	Geological Unit	Rock type	Age (Ma)	Error (\pm Ma)	Method	Material	Reference
7	SR44	6.340	75.580	AB	Quartzdiorite	26.6	1.3	U-Th/He	Apatite	9
4	SR45	6.360	75.590	AB	Quartzdiorite	45.7	2.3	U-Th/He	Apatite	9
12	SR46	6.360	75.590	AB	Quartzdiorite	40.8	2	U-Th/He	Apatite	9
6	SR48	6.350	75.580	AB	Quartzdiorite	32.2	1.6	U-Th/He	Apatite	9
40	SR6	6.430	75.370	AB	Quartzdiorite	33.7	1.7	U-Th/He	Apatite	9
13	SR9	6.460	75.370	AB	Quartzdiorite	43.6	2.2	U-Th/He	Apatite	9
26	SRCC1	6.860	75.180	AB	Quartzdiorite	22.8	1.1	U-Th/He	Apatite	9
81	SRCC2	6.800	75.140	AB	Quartzdiorite	23.9	1.2	U-Th/He	Apatite	9
29	SRCC3	6.760	75.120	AB	Quartzdiorite	24.2	1.2	U-Th/He	Apatite	9
57	WR200	6.038	74.746	LCS	Tonalite	87.5	1.3	U-Pb (LA)	Zircon	5
21	WR201	6.852	75.329	AB	Tonalite	75.1	1.3	U-Pb (LA)	Zircon	5
80	WR202	6.789	75.202	AB	Diorite	84.2	2.3	U-Pb (LA)	Zircon	5
63	WR221	6.509	74.878	AB	Quartzdiorite	87.4	1.3	U-Pb (LA)	Zircon	5
22	WR305	6.825	75.460	AB	Tonalite	73.9	1.3	U-Pb (LA)	Zircon	5
76	DV148	6.421	75.385	AB	Granodiorite	53	4.8	FT	Apatite	13
55	DV153	6.540	75.122	AB	Granodiorite	66.6	8	FT	Zircon	13
44	DV56	6.056	75.212	AB	Granite	40.1	1	U-Th/He	Zircon	14
44	DV56	6.056	75.212	AB	Granite	40.2	2.6	U-Th/He	Zircon	13
44	DV56	6.056	75.212	AB	Granite	65.5	6	FT	Zircon	13
70	DV63	5.978	74.959	AB	Aplite	20.6	1.4	U-Th/He	Apatite	13
70	DV63	5.978	74.959	AB	Aplite	20.9	1.2	U-Th/He	Apatite	14
70	DV63	5.978	74.959	AB	Aplite	64.1	9.6	FT	Apatite	13
72	DV64	5.982	74.955	AB	Granodiorite	58.9	9.6	Ar/Ar	Plagioclase	13
72	DV64	5.982	74.955	AB	Granodiorite	59.8	10.2	FT	Apatite	13
72	DV64	5.982	74.955	AB	Granodiorite	62.6	0.7	Ar/Ar	Plagioclase	13
17	DV70	6.971	75.426	AB	Granodiorite	39.1	2.1	U-Th/He	Apatite	13
17	DV70	6.971	75.426	AB	Granodiorite	54.8	5.8	FT	Apatite	13
17	DV70	6.971	75.426	AB	Granodiorite	58.1	5.2	FT	Zircon	13
17	DV70	6.971	75.426	AB	Granodiorite	68.6	1.5	Ar/Ar	Biotite	13
17	DV70	6.971	75.426	AB	Granodiorite	68.9	0.6	Ar/Ar	Biotite	13
83	JPZ-178	6.744	75.7900	SQ	Quartzdiorite	71.6	1.2	U-Pb (LA)	Zircon	19
84	MGO-238	6.772	75.774	SQ	Quartzdiorite	71.9	1.9	U-Pb (LA)	Zircon	19

Abbreviation: **FID:** Figure Identification number; *Decimal degrees; **AB:** Antioqueño Batholith; **US:** La Unión Stock; **OB:** Ovejas Batholith; **AS:** Altavista Stock; **MLS:** Media Luna Stock; **LCS:** La Culebra Stock; **Q:** Aluvial deposit; **V:** Volcanic deposit; **ERP:** El Rayo porphyry intrusive; **CS:** Caracolí Stock; **LV:** El Limón vein; **SQ:** Sabanalarga Quartzdiorite; **FT:** Fission Tracks; **U-Pb (LA):** U-Pb LA-MC-ICP-MS; **TIMS:** U-Pb ID-TIMS; **SHRIMP:** U-Pb SHRIMP.

References: **1.** Botero and González, 1983; **2.** Feininger and Botero, 1982; **3.** Fujiyoshi *et al.*, 1976; **4.** Ibáñez Mejía, 2011; **5.** Leal Mejía, 2011; **6.** Ordóñez Carmona and Pimentel, 2001; **7.** Ordóñez Carmona, 1997; **8.** Pérez, 1967; **9.** Restrepo Moreno *et al.*, 2009; **10.** Restrepo, 1991; **11.** Sáenz *et al.*, 1996; **12.** Toro *et al.*, 2006; **13.** Villagómez and Spikings, 2013; **14.** Villagómez, 2010; **15.** Villagómez *et al.*, 2011; **16.** Correa *et al.*, 2006; **17.** Cochrane, *et al.*, 2014; **18.** Restrepo, *et al.*, 2012; **19.** Zapata *et al.*, 2017.

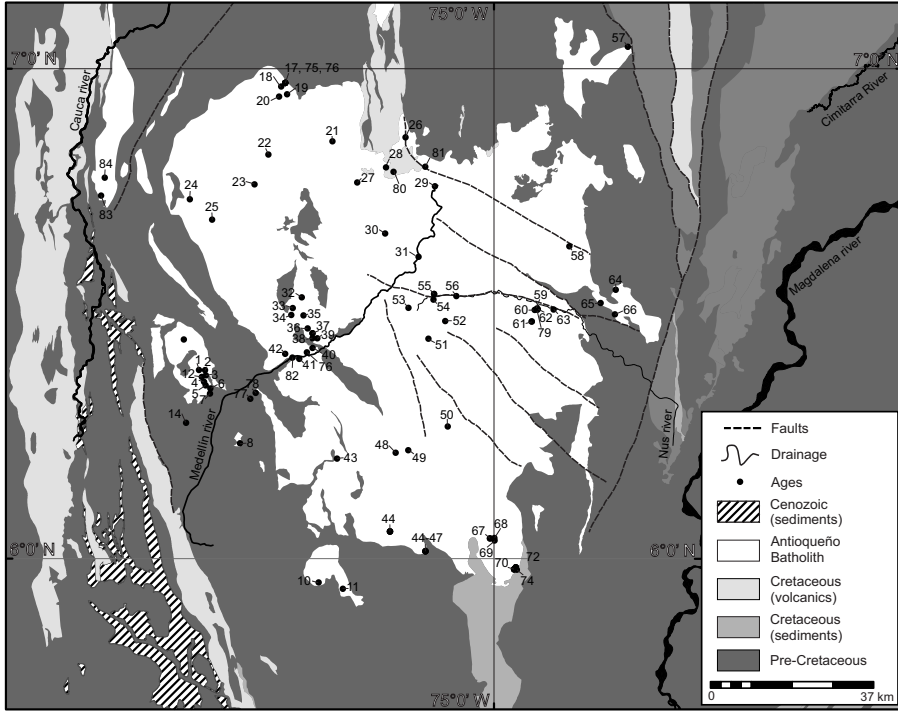


FIG. 2. Summary of geochronological ages (Ma) obtained for the Antioquia Batholith and satellite bodies using different methods. Data from table 1.

95 and 87 Ma located to the south of the batholith, including the San Diego and Altavista stocks; (ii) a second pulse between 89 and 82 Ma, mainly located on the margins of the pluton, including La Culebra and a more felsic facies of the Altavista stocks; (iii) a third pulse between 81 and 72 Ma that includes the Ovejas stock; (iv) the fourth and youngest pulse of Eocene age (~63 to 58 Ma) is identified in the central-eastern portion of the batholith (Fig. 3B). This last magmatic pulse is also correlatable with other plutons located south on the Central Cordillera such as Hatillo, Manizales, El Bosque, Norcasia and Sonsón (Bayona *et al.*, 2012; Bustamante *et al.*, 2017) and the Santa Marta batholith and the Parashi stock located at the Colombian caribbean (Cardona *et al.*, 2011; Cardona *et al.*, 2014; Salazar *et al.*, 2016).

3. Methods

3.1. U-Pb geochronology

This paper presents five new U-Pb (LA-ICP-MS) ages in zircon (crystallization ages) from La

Unión Stock and Ovejas Batholith. These ages were obtained at the Laboratorio de Estudios Isotópicos (LEI), Centro de Geociencias (CGEO), Universidad Nacional Autónoma de México (UNAM) following procedures described in Solari *et al.* (2010). Zircon crystals were separated using conventional techniques of rock crushing, sieving, Frantz isodynamic magnetic separator, panning, and heavy liquid separation. Crystal ablation was performed using an ArF excimer laser (Resolution M-50) operated at 193nm, 5 Hz and ~6 J/cm. The Plešovice reference zircon (*ca.* 337 Ma; Sláma *et al.*, 2008) was used in combination with NIST 610 standard glass to correct for instrumental drift and down-hole fractionation and to recalculate elemental concentrations, using the UPb.age script for R (Solari and Tanner, 2011) and Iolite (Paton *et al.*, 2010). Because its signal is swamped by the ^{204}Hg contained in the carrier gases, ^{204}Pb was not analyzed during this study. Common Pb correction, where needed, was thus performed employing the algebraic method of Andersen (2002). Concordia and age distribution plots, as well as age error calculations, were performed using Isoplot v. 3.70 (Ludwig, 2004).

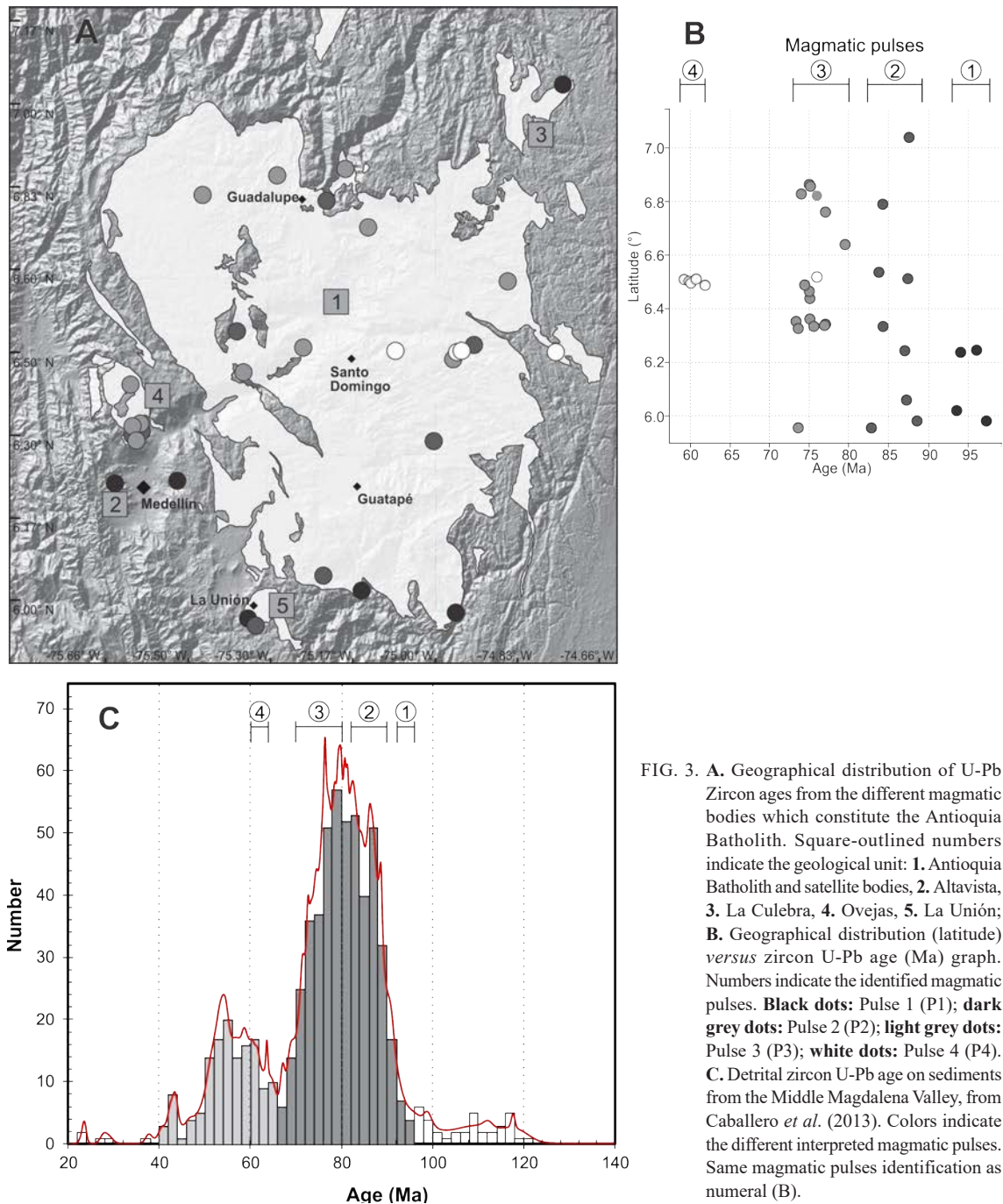


FIG. 3. A. Geographical distribution of U-Pb Zircon ages from the different magmatic bodies which constitute the Antioquia Batholith. Square-outlined numbers indicate the geological unit: 1. Antioquia Batholith and satellite bodies, 2. Altavista, 3. La Culebra, 4. Ovejas, 5. La Unión; B. Geographical distribution (latitude) versus zircon U-Pb age (Ma) graph. Numbers indicate the identified magmatic pulses. Black dots: Pulse 1 (P1); dark grey dots: Pulse 2 (P2); light grey dots: Pulse 3 (P3); white dots: Pulse 4 (P4). C. Detrital zircon U-Pb age on sediments from Caballero *et al.* (2013). Colors indicate the different interpreted magmatic pulses. Same magmatic pulses identification as numeral (B).

3.2. Whole-rock geochemistry

Whole rock geochemistry was performed on the same samples where U-Pb ages were obtained, except for the A.G.1.6 sample (La Unión Stock),

which was completely weathered. Major elements analysis were performed by X-ray fluorescence with a Siemens SRS-300 equipment, following the procedures described by Lozano-Santa Cruz *et al.* (1995). Trace elements analysis were performed

on the LEI by ICP-MS using a Thermo Series XII equipment, under procedures described by Mori *et al.* (2009). Two additional digestion steps were added in order to achieve complete dissolution of highly refractory minerals (*e.g.*, zircon) as described in Duque-Trujillo *et al.* (2014).

Due to the impossibility of accessing raw data from Leal-Mejía (2011) a graphic comparison was made between the data of this author and the data here presented.

4. Results

4.1. Petrography and geochemistry

Petrographic analyses were performed on four samples from the Ovejas Batholith and one sample from a magmatic mafic enclave. The sample belonging to La Unión Stock could not be analyzed due to its high degree of weathering.

The analyzed samples were classified as granodiorites. Broadly speaking, the samples are hypidiomorphic, equigranular, coarse to medium grained. These are mainly composed of quartz, plagioclase, K-feldspar, hornblende, and biotite. Magmatic mafic enclaves are common, and those present the same mineralogical composition as the main magmatic mass with a high content of mafic minerals.

Plagioclase is usually classified as andesine although compositional zonation is frequent. K-feldspar is classified as orthoclase. The amphibole, classified as hornblende, usually presents a genetic relationship with biotite in clusters of crystals. The amphibole and biotite are frequently altered to chlorite and present local replacements to epidote-clinozoisite. These observations agree with the results obtained by Feininger and Botero (1982) and Álvarez (1983) for the Antioquia Batholith. Those authors, based on a large data-set, found that the petrographic characteristics of the main granitic mass of the Antioquia Batholith are very homogeneous, with a ~97% of the samples classified as granodiorites to tonalities.

Four samples of the Ovejas Batholith were geochemically analyzed and their results are presented in table. 2. Three samples correspond to the main granodioritic mass of the Ovejas Batholith and one sample from a mafic enclave. Samples belonging to the granodioritic mass were classified as quartz-diorites and diorites, meanwhile the mafic enclave

fall in the gabbro field (Fig. 4A). SiO_2 vary from 61.9 to 66.7 wt%, while K_2O content is almost invariant around ~1.8 wt% for the granitic samples, which fall in the calc-alkaline series of medium K (Fig. 4B). The mafic enclave has 52.3% of Si_2O and higher K_2O , locating the sample on the Shoshonitic series. MgO values range from 1.5 to 2.3 wt% in the granitic samples, and have a value of 4.1 wt% for the mafic enclave. Al_2O_3 values range from 16.2 to 17.0 wt% within the granitic samples, and 17.9 wt% for the mafic enclave. From the four analyzed samples, two samples, (the mafic enclave and one granitic sample) fall in the metaluminous field, meanwhile the other two granitic rocks fall into the peraluminous field (Fig. 4C).

Primitive mantle-normalized multi-element diagrams for the Ovejas Batholith rocks are characterized by an enrichment of the Large Ion Lithophile Elements (LILE) over the High Field Strength Elements (HFSE) (Fig. 5A, C). These patterns are also characterized by negative Nb-Ta, La-Ce and Ti anomalies, and positive Pb, and Zr-Hf anomalies (Fig. 5A, C). Although the mafic enclave has a similar pattern as the granitic rocks, it differs from those in some aspects, especially those related to less differentiated rocks (*e.g.*, Zr-Hf anomaly, which is negative in the mafic enclave and positive in the granitic rocks).

Chondrite-normalized REE patterns show a well-defined LREE enrichment ($[\text{La}/\text{Yb}]_{\text{N}}$ ratios vary from 6.4 to 8.6 in granitic rocks and 3.8 for the mafic enclave) and an almost flat HREE pattern ($[\text{Gd}/\text{Yb}]_{\text{N}}$ ratios vary from 1.58 to 1.70 in granitic rocks and 1.51 for the mafic enclave) (Fig. 5B, D, E and F). Unless all samples have similar patterns, La/Yb ratios show that the mafic enclave rock is less depleted in REE than the granitic samples (Fig. 5B, D and E). Eu anomaly is present in three from the four analyzed samples (Fig. 5B). The mafic enclave shows a well-defined negative anomaly ($\text{Eu}/\text{Eu}^*=0.68$), meanwhile the granitic rocks all samples have positive anomalies (Eu/Eu^* from 1.03 to 1.42) (Fig. 5G).

4.2. U-Pb geochronology

Zircon U-Pb crystallization ages (Table 3) were obtained by the LA-ICP-MS method in five samples (Fig. 6 and 7). One of them corresponds to the La Unión Stock, and four to the Ovejas Batholith. In

TABLE 2. GEOCHEMISTRY DATA FROM THE ANALYZED SAMPLES.

Sample	AG14B	AG12	AG13	AG14
Geological Unit	Ovejas Batholith	Ovejas Batholith	Ovejas Batholith	Ovejas Batholith
Age (Ma)		75.48±0.95	76.9±2.5	74.3±1.9
Latitude (N)	6.325250°	6.331278°	6.331664°	6.325250°
Longitude (W)	-75.597114°	-75.601819°	-75.598747°	-75.597114°
Major Elements in wt%				
SiO ₂	52.32	66.72	65.66	61.99
TiO ₂	1.15	0.48	0.486	0.677
Al ₂ O ₃	17.89	16.21	16.96	17.02
Fe ₂ O ₃	10.25	4.06	4.28	5.9
MnO	0.24	0.094	0.111	0.126
MgO	4.16	1.49	1.53	2.28
CaO	6.19	3.72	3.97	5.22
Na ₂ O	3.58	4.1	4.18	3.71
K ₂ O	2.69	1.86	1.92	1.83
P ₂ O ₅	0.22	0.122	0.117	0.166
LOI	0.49	0.4	0.32	0.37
Total	99.2	99.3	99.5	99.3
Trace Elements in ppm				
Li	41.21	27.76	22.21	23.65
Be	1.36	1.39	1.02	1.18
Mg	3.98	1.4	1.34	2.14
P	0.275	0.147	0.129	0.197
Ca	6.01	3.74	3.94	5.23
Sc	21.2	3.62	5.16	9.55
Ti	1.16	0.46	0.46	0.641
V	150.75	40.12	39.14	83.76
Cr	23.09	22.78	18.37	21.85
Mn	0.246	0.084	0.1	0.120
Fe	10.18	3.94	4.21	5.8
Co	15.89	5.24	5.39	9.21
Ni	6.01	5.06	4.01	4.18
Cu	6.92	5.9	4.84	5.59
Zn	141.17	78.41	81.48	80.93
Ga	23.13	19.14	20	20.1
Rb	87.48	43.1	48.14	49.48
Sr	298.46	331.42	353.41	349.4
Y	33.7	9.67	10.85	16.63
Zr	124.99	164.36	135.94	108.44

table 2 continued.

Sample	AG14B	AG12	AG13	AG14
Geological Unit	Ovejas Batholith	Ovejas Batholith	Ovejas Batholith	Ovejas Batholith
Age (Ma)		75.48±0.95	76.9±2.5	74.3±1.9
Latitude (N)	6.325250°	6.331278°	6.331664°	6.325250°
Longitude (W)	-75.597114°	-75.601819°	-75.598747°	-75.597114°
Nb	11.35	8.75	9.36	7.06
Mo	-0.08	-0.16	-0.08	-0.15
Sn	2.48	1.53	1.64	1.33
Sb	0.08	0.07	0.09	0.09
Cs	2.67	1.78	2.05	1.69
Ba	810.1	739.26	675.62	665.98
La	17.68	8.12	9.05	19.22
Ce	40.52	15.16	16.22	32.5
Pr	5.81	2.14	2.14	4.19
Nd	24.72	8.5	8.41	15.05
Sm	5.81	1.9	1.9	3.08
Eu	1.32	0.884	0.869	1.05
Tb	0.959	0.286	0.297	0.483
Gd	5.98	1.87	1.9	3.07
Dy	5.49	1.59	1.7	2.78
Ho	1.11	0.312	0.343	0.553
Er	3.32	0.888	0.974	1.63
Yb	3.28	0.908	0.995	1.6
Lu	0.505	0.150	0.165	0.256
Hf	3.11	3.83	3.24	2.58
Ta	0.823	0.724	0.716	0.652
W	0.631	0.101	0.077	0.140
Tl	0.784	0.508	0.500	0.492
Pb	6.67	6.27	6.88	6.2
Th	4.98	4.03	3.74	5.98
U	0.925	1.13	1.38	1.18

order to obtain the age of the last crystallization event, the preferred ablation target were crystal borders; nevertheless, some cores were analyzed in order to identify possible inherited ages.

4.2.1. La Unión Stock

One sample (AG 1.6) was analyzed for this pluton. Cathodoluminescence (CL) images show

thin concentric overgrowths around ante-crystals (Fig. 6). Twenty-six analysis from this sample yield a weighted mean $^{238}\text{U}/^{206}\text{Pb}$ age of 97.2 ± 0.6 Ma (Fig. 6). This age is dominated by the age of the magmatic overgrowths, leading to interpret this as the age of the latest magmatic activity during the La Unión Stock magmatism. Zircon cores yield ages only ~4 Ma older than the overgrowths (102-100 Ma).

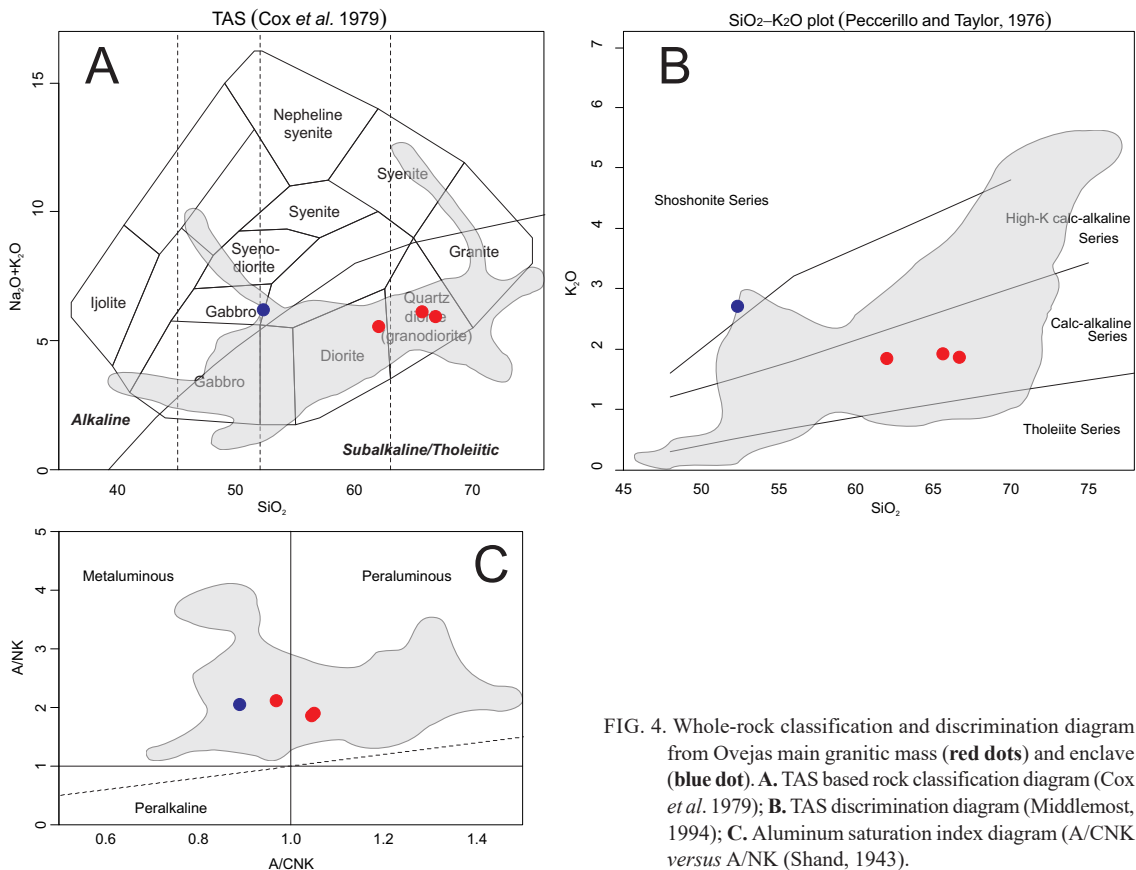


FIG. 4. Whole-rock classification and discrimination diagram from Ovejas main granitic mass (red dots) and enclave (blue dot). A. TAS based rock classification diagram (Cox et al. 1979); B. TAS discrimination diagram (Middlemost, 1994); C. Aluminum saturation index diagram (A/CNK versus A/NK (Shand, 1943).

4.2.2. Ovejas Batholith

Four samples were analyzed for the Ovejas Batholith (AG 1.1, 1.2, 1.3 and 1.4) (Fig. 3). CL-images show mostly thin concentric overgrowths around an older core (Fig. 7). Although most of the analytical spots were located on zircons overgrowths, some of them were located on the cores (Fig. 7). Single-spot U-Pb ages obtained from the Ovejas Batholith samples yield ages between 85 and 66 Ma (Fig. 7); meanwhile, intercept ages fall between 76.9 and 73.3 Ma (Fig. 7). A weighted mean age calculated using those four ages yield an age of 75.2 Ma (MSWD=0.47).

Although intercept ages from the Ovejas Batholith clearly define a coherent unique age for this magmatism, sample AG 1.1 has three zircons with ages ~10 M.y. younger (66-62 Ma) than the intercept age calculated for that sample. It is plausible that these zircons represent a later magmatic pulse

which had affected part of the Ovejas Batholith between 66 and 64 Ma.

5. Discussion

5.1. The length of the upper Cretaceous to Eocene arc magmatism in the Northern Andes and its tectonic setting

Our new U-Pb crystallization ages from La Unión stock (*ca.* 97 Ma) and Ovejas Batholith (*ca.* 76 to 73 Ma), together with ages previously reported for the Antioquia batholith and its satellite bodies (Ordóñez-Carmona et al., 2006; Correa et al., 2006; Restrepo-Moreno et al., 2007; Ibáñez-Mejía et al., 2007; Leal-Mejía, 2011; Villagómez et al., 2011) ranging from *ca.* 89 to 58 Ma, suggest that after ~20 m.y. of magmatic quiescence, continental arc magmatism resumed during upper Cretaceous in

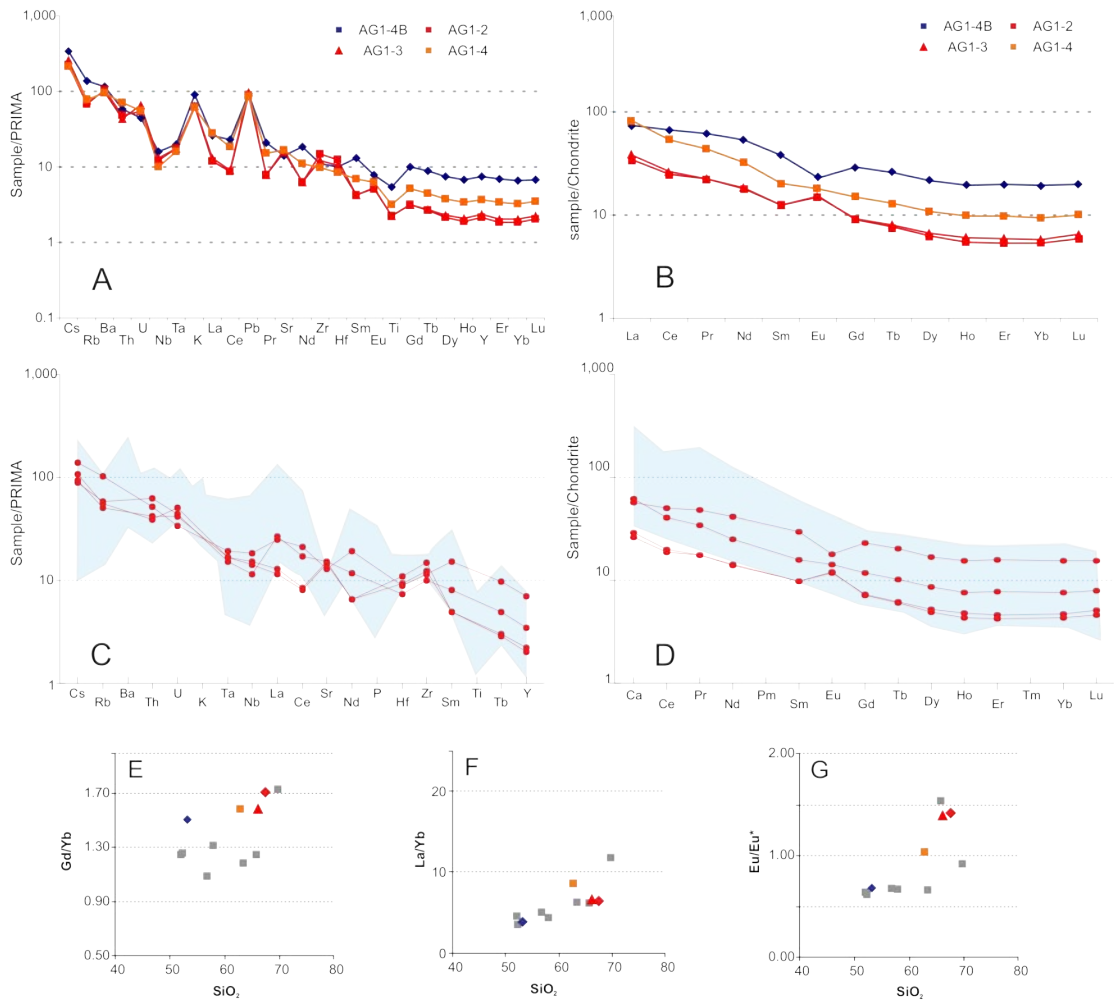


FIG. 5. Trace element diagrams for samples from ovejas Batholith (in red) and mafic enclave (in blue). **A.** Trace element (PRIMA normalized, Wood, 1979); **B.** REE normalized diagram (normalized using Boynton, 1984) spider-diagram from the Ovejas Batholith; **C-D.** Ovejas Batholith trace elements spider-diagrams compared with Leal-Mejía (2011); Antioquia Batholith data; **E-G.** Trace elements ratio for the Ovejas Batholith and Antioquia Batholith from Almeida and Villamizar (2012) in grey color.

TABLE 3. GEOCHRONOLOGICAL DATA FROM ANALYZED SAMPLES.

Sample	Latitude	Longitude	m a.s.l.	Age (Ma)	Error (Ma)	Inherited crystals (Ma)
Ovejas Batholith						
AG 1.4	6.3252°	-75.5971°	2,343	74.3	1,9	85
AG 1.3	6.3316°	-75.5987°	2,400	76.9	2.5	92-86
AG 1.2	6.3312°	-75.6018°	2,411	75.5	1	-
AG 1.1	6.3488°	-75.6087°	2,479	73.3	2.4	-
La Unión Stock						
AG 1.6	5.9770°	-75.3675°	2,493	97.2	1	-

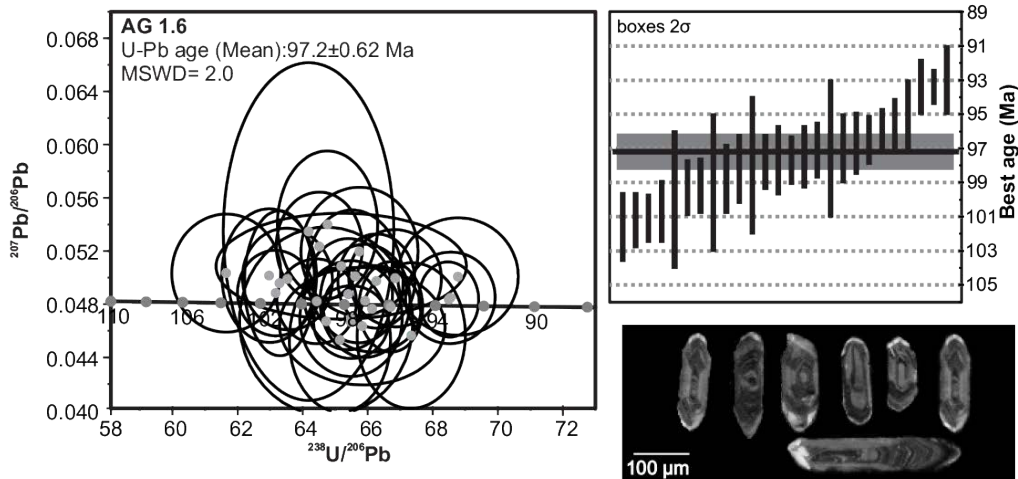


FIG. 6. U-Pb zircon (LA-ICP-MS) geochronology results from La Unión Pluton.

the Central Cordillera and lasted until the Eocene. Age distribution in the Antioquia batholith (Fig. 3) suggests that it was constructed from south to north, with a most voluminous period of magmatism between 89 and 72 Ma. However, despite the apparent 40 m.y. of continuous magmatism in the Central Cordillera, a clear gap between 72 and 63 Ma is present as seen in figure 3C and in the detrital record (U-Pb in zircon) of sedimentary basins from eastern Colombia, where two group ages (Late Cretaceous and Paleogene) are abundant, whereas the ~62 to 70 m.y. ages are scarcely represented. It is noteworthy than the Antioquia Batholith is until now, the only vestige of late Cretaceous arc-related magmatism in the Central Cordillera. Conversely, the Paleogene magmatism is extended along the Central Cordillera (Bustamante *et al.*, 2017) and the Caribbean region (Cardona *et al.*, 2012, 2014).

According to such age distribution exposed over the present work, we propose to challenge previous geological models which suggest a southward magmatic migration during Paleogene (Ordóñez *et al.*, 2001; Cardona *et al.*, 2012; Pindell and Kennan, 2009; Pindell *et al.*, 1998, 2006). Instead, we propose that continental arc magmatism was stationary during upper Cretaceous, forming the Antioquia Batholith, whereas its Paleogene pulse, ~10 Ma after the mentioned magmatic hiatus, was formed on the eastern side and share geochemical features with other Paleogene post-collisional plutons of the Central Cordillera (Bustamante *et al.*, 2017). Further Miocene

rotation of the Sierra Nevada de Santa Marta located northern of Colombia (Montes *et al.*, 2010) and the oblique convergence between South America and the Caribbean Plate may have dispersed the Eocene granitoids from its former position (Cardona *et al.*, 2014), which in turn, may explain the magmatic gap between the Central Cordillera and the Sierra Nevada de Santa Marta (Fig. 1). The coincidence of the aforementioned ~10 m.y. magmatic hiatus with increasing Sr/Y ratios, suggest that the collision of the Caribbean plateau with NW South America may have caused such period of magmatic quiescence.

Whole rock geochemical results from the Ovejas Batholith indicate an arc related setting for this pluton according to the Nb, Ti and Ta negative anomalies (Fig. 5) as well as the LREE/HREE ratios ($[La/Yb]_N$ from 6.4 to 8.6). We compared our results with geochemical analyses obtained in previous works of the Antioquia Batholith (Botero, 1963; Feininger and Botero, 1982; González, 1980; Álvarez, 1983; Sáenz, *et al.*, 2003; Villagómez, 2010; Almeida and Villamizar, 2012). Such compilation, however, lacks of the raw data and trace and REE analyses, and only eight of them are complete (Almeida and Villamizar, 2012). Analytical data obtained by Leal-Mejía (2011) are also included in this compilation by graphical comparison because the absence of the raw data.

Primordial mantle-normalized trace-element trends exhibit a clear enrichment in LILE over HFSE (Fig. 5A) with similar patterns as the obtained for the Ovejas Batholith. This can be compared in figure 5C

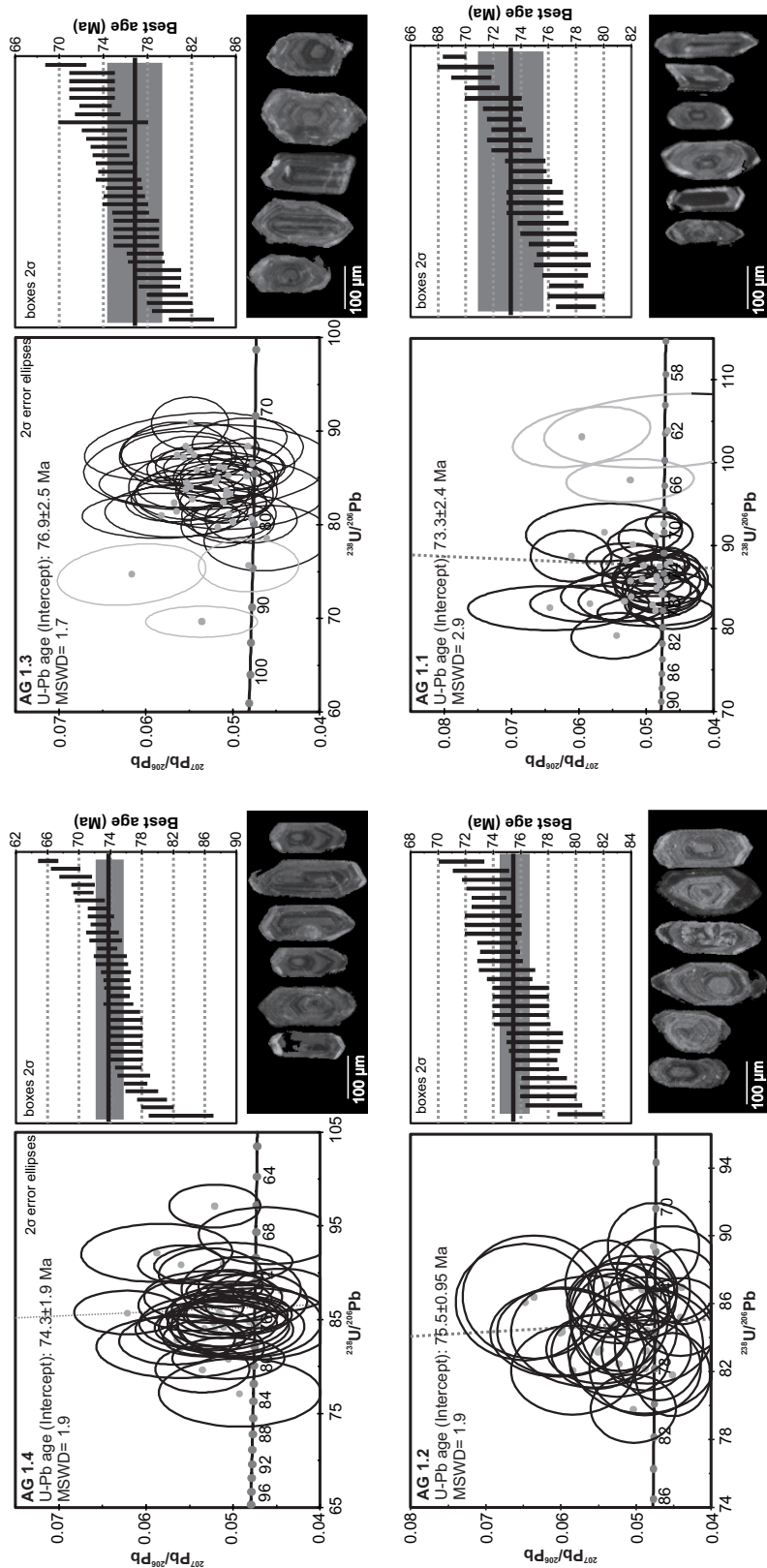


FIG. 7. U-Pb zircon (LA-ICP-MS) geochronology results from Ovejas batholith.

and by the $[La/Yb]_{\text{IN}}$ ratio values in figure 5F. Nb, Ta and Ti negative anomalies, and Zr, Hf positive anomalies are identifiable (Fig. 5A). Chondrite-normalized REE patterns show enrichment in LREE *versus* HREE with similar patterns as those obtained for the Ovejas Batholith. Nevertheless, Antioquia batholith has less steep MREE-HREE patterns, indicated by the Gd/Yb ratio.

Some authors consider these and other plutons in Aruba, Curaçao, Pujilí, Guajira, among others, as belonging to the tonalite-trondhjemite-granodiorite series or having an adakitic affinity (e.g., Wright and Wyld, 2011; Whatam and Stern, 2015). Pindell and Kennan (2009) consider that this series of plutons are so close to the Caribbean-South American Plate boundary and cast doubt on the normal arc setting for these rocks, suggesting the melting of a slab-tip during subduction initiation. Conversely, we claim for a primitive continental arc setting for the Antioquia batholith and its satellite bodies based on the aforementioned geochemical evidences. Such magmatic arc is recording an increasing in its maturity with time as suggested in the Rb/Zr *versus* Nb ratios (Fig. 8). Elliot *et al.* (1997) observed that incompatible elements like Ba and Th can be used as tracers of fluids derived from subducting slabs. In that sense, the high Ba/Th (~111 to 185) ratios of

the Antioquia batholith are indicative of a continental arc where the slab derived fluids are increasing with maturity (Fig. 8). The stationary character of the magmatism represented by the Antioquia batholith, indicates that the subduction components (hydrous fluids) involved in the petrogenesis of these magmas would have changed locally, and are not related to the migration of the magmatic arc away from the trench.

6. Conclusions

Syn- to post-collisional tectonics characterized the NW margin of South America since the Late Cretaceous to the Eocene, mainly influenced by the interaction of the Farallón and Caribbean plates with this margin. The Antioquia batholith, built by successive magmatic pulses for *ca.* 40 m.y., constitutes one of the main magmatic records of this tectonic scenario. Its crystallization history can be inferred according to new and already published U-Pb ages, whereas the whole rock geochemistry suggests that this magmatism is arc-related and that its locus may have been relatively stationary since no evidences of arc migration are recorded.

The latest magmatic phases of the Antioquia Batholith, Paleogene in age, constitute part of a magmatic arc that includes other small volume

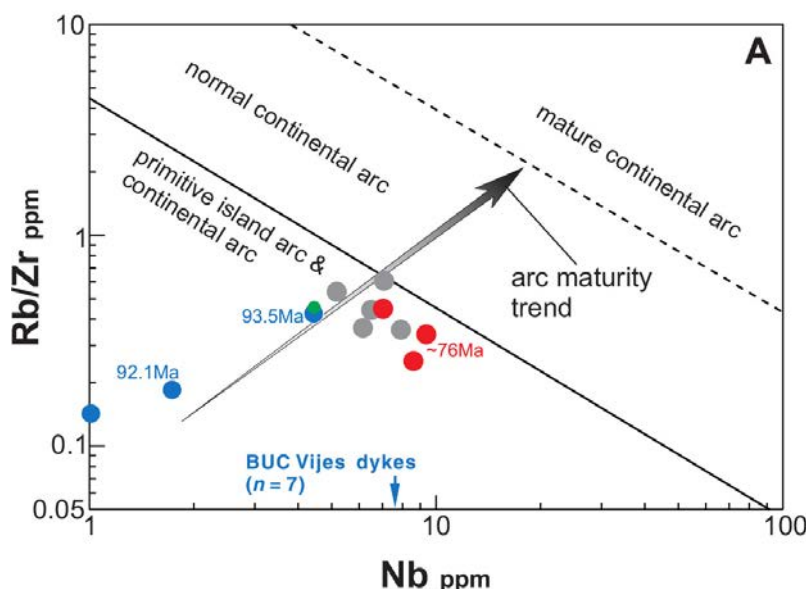


FIG. 8. Rb/Zr *versus* Nb diagram (Brown *et al.*, 1984). Data from samples belonging to the Antioquia batholith from: Whatam and Stern (2015), blue dots; Almeida and Villamizar (2012), red dots; Villagómez (2010), green dots; this work, gray dots.

plutons currently located at the Colombian Caribbean. This formerly arc would have been disrupted and dispersed by the interaction between the NW margin of South America and the Caribbean Plate which lead to rotation and translation of cortical blocks as well as basin formation.

Acknowledgements

The authors would like to thank C. Ortega Obregón and O. Pérez Arvizu from Laboratorio de Estudios Isotópicos (LEI) and J.T. Vázquez from CGEO, UNAM for their help during sample treatment. U. Cordani, A. Cardona and W. Vivallo are acknowledged for their constructive reviews that help to improve the manuscript.

References

- Almeida, J.; Villamizar, F. 2012. Petrografía y geoquímica del Batolito Antioqueño en un sector del Municipio de Santa Rosa de Osos, Antioquia. Tesis de grado, Universidad Industrial de Santander: 216 p.
- Álvarez, A. 1983. Geología de la Cordillera Central y el Occidente colombiano y petroquímica de los intrusivos granitoides Meso-Cenozoicos. Instituto Nacional de Investigaciones Geológico-Mineras 26 (2):1-175.
- Andersen, T. 2002. Correction of common lead in U-Pb analyses that do not report ^{204}Pb . Chemical Geology 192 (1): 59-79.
- Annen, C.; Blundy, J.D.; Leuthold, J.; Sparks, R.S.J. 2015. Construction and evolution of igneous bodies: Towards an integrated perspective of crustal magmatism. Lithos 230: 206-221.
- Aspden, J.A.; McCourt, W.J.; Brook, M. 1987. Geometrical control of subduction-related magmatism: the Mesozoic and Cenozoic plutonic history of Western Colombia. Journal of the Geological Society 144 (6): 893-905.
- Bayona, G.; Cardona, A.; Jaramillo, C.; Mora, A.; Montes, C.; Valencia, V.; Ayala, C.; Ibáñez-Mejía, M. 2012. Early Paleogene magmatism in the northern Andes: Insights on the effects of Oceanic Plateau-continent convergence. Earth and Planetary Science Letters 331: 97-111.
- Best, M.G. 2013. Igneous and metamorphic petrology. John Wiley and Sons: 729 p.
- Bissig, T.; Leal-Mejía, H.; Stevens, R.B.; Hart, C.J. 2017. High Sr/Y Magma Petrogenesis and the Link to Porphyry Mineralization as Revealed by Garnet-Bearing I-Type Granodiorite Porphyries of the Middle Cauca Au-Cu Belt, Colombia. Economic Geology 112 (3): 551-568.
- Blanco-Quintero, I.F.; García-Casco, A.; Toro, L.M.; Moreno, M.; Ruiz, E.C.; Vinasco, C.J.; Cardona, A.; Lázaro, C.; Morata, D. 2014. Late Jurassic terrane collision in the northwestern margin of Gondwana (Cajamarca Complex, eastern flank of the Central Cordillera, Colombia). International Geology Review 56 (15): 1852-1872.
- Botero, G. 1963. Contribución al conocimiento de la zona central de Antioquia. Universidad Nacional de Colombia. Anales Facultad de Minas 57: 1-101. Medellín.
- Botero, G.A.; González, H. 1983. Algunas localidades fosilíferas cretácicas de la Cordillera Central. Antioquia y Caldas, Colombia Norandina 7: 15-27.
- Boynton, W.V.Z. 1984. Geochemistry of the rare earth elements: meteorite studies. Rare earth element geochemistry. Elsevier: 63-114.
- Brown, G.C.; Thorpe, R.S.; Webb, P.C. 1984. The geochemical characteristics of granitoids in contrasting arcs and comments on magma sources. Journal of the Geological Society of London 141: 413-426.
- Bustamante, C.; Archanjo, C.J.; Cardona, A.; Vervoort, J. D. 2016. Late Jurassic to Early Cretaceous plutonism in the Colombian Andes: A record of long-term arc maturity. Geological Society of America Bulletin 128 (11-12): 1762-1779.
- Bustamante, C.; Cardona, A.; Archanjo, C.J.; Bayona, G.; Lara, M.; Valencia, V. 2017. Geochemistry and isotopic signatures of Paleogene plutonic and detrital rocks of the Northern Andes of Colombia: A record of post-collisional arc magmatism. Lithos 277: 199-209.
- Caballero, V.; Mora, A.; Quintero, I.; Blanco, V.; Parra, M.; Rojas, L.E.; López, C.; Sánchez, N.; Horton, B.K.; Stockli, D.; Duddy, I. 2013. Tectonic controls on sedimentation in an intermontane hinterland basin adjacent to inversion structures: The Nuevo Mundo syncline, Middle Magdalena Valley, Colombia. Geological Society, Special Publications 377 (1): 315-342. London.
- Cardona, A.; Valencia, V.; Bustamante, C.; García-Casco, A.; Ojeda, G.; Ruiz, J.; Saldarriaga, M.; Weber, M. 2010. Tectonomagmatic setting and provenance of the Santa Marta Schists, northern Colombia: Insights on the growth and approach of Cretaceous Caribbean oceanic terranes to the South American continent. Journal of South American Earth Sciences 29 (4): 784-804.
- Cardona, A.; Valencia, V.A.; Bayona, G.; Duque, J.; Ducea, M.; Gehrels, G.; Jaramillo, C.; Montes, C.; Ojeda, G.; Ruiz, J. 2011. Early-subduction-related orogeny in the northern Andes: Turonian to Eocene

- magmatic and provenance record in the Santa Marta Massif and Ranchería Basin, northern Colombia. *Terra Nova* 23 (1): 26-34.
- Cardona, A.; Montes, C.; Ayala, C.; Bustamante, C.; Hoyos, N.; Montenegro, O.; Ojeda, C.; Niño, H.; Ramírez V.; Valencia, V.; Rincón, D.; Vervoort, J.; Zapata, S. 2012. From arc-continent collision to continuous convergence, clues from Paleogene conglomerates along the southern Caribbean-South America plate boundary. *Tectonophysics* 580: 58-87.
- Cardona, A.; Weber, M.; Valencia, V.; Bustamante, C.; Montes, C.; Cordani, U.; Muñoz, C. M. 2014. Geochronology and geochemistry of the Parashi granitoid, NE Colombia: Tectonic implication of short-lived Early Eocene plutonism along the SE Caribbean margin. *Journal of South American Earth Sciences* 50: 75-92.
- Cochrane, R.; Spikings, R.; Gerdes, A.; Winkler, W.; Ulianov, A.; Mora, A.; Chiaradia, M. 2014. Distinguishing between in-situ and accretionary growth of continents along active margins. *Lithos* 202: 382-394.
- Coleman, D.S.; Gray, W.; Glazner, A.F. 2004. Rethinking the emplacement and evolution of zoned plutons: Geochronologic evidence for incremental assembly of the Tuolumne Intrusive Suite, California. *Geology* 32 (5): 433-436.
- Correa, M.; Pimentel, M.; Restrepo, J.J.; Nilson, A.; Ordoñez, O.; Martens, U.; Laux, U.; Junges, S. 2006. U-Pb zircon ages and Nd-Sr isotopes of the Altavista stock and the San Diego gabbro: New insights on Cretaceous arc magmatism in the Colombian Andes. In *South American Symposium on Isotope Geology*, No. 5: 84-86. Montevideo.
- Cox, K.; Bell, J.; Pankhurst, R. 1979. The interpretation of igneous rocks. Allen and Unwin, London: 450 p.
- Duque-Trujillo, J.; Ferrari, L.; Orozco-Esquível, T.; López-Martínez, M.; Lonsdale, P.; Bryan, S.E.; Kluesner, J.; Piñero-Lajas, D.; Solari, L. 2014. Timing of rifting in the southern Gulf of California and its conjugate margins: Insights from the plutonic record. *Geological Society of America Bulletin* 127 (5-6): 702-736. doi: 10.1130/B31008.1.
- Elliot, T.; Plank, T.; Zindler, A.; White, W.; Bourdon, B. 1997. Element transport from slab to volcanic front at the Mariana arc. *Journal of Geophysical Research* 102: 14991-15019.
- Feininger, T.; Botero, G. 1982. The Antioquian Batholith, Colombia. INGEOMINAS. Publicaciones Geológicas Especiales del INGEOMINAS 12: 1-150. Bogotá.
- Fujiyoshi, A.; Ishizaka, K.; Hayase, I.; Tokuyama, A. 1976. Metamorphic and igneous rocks from Medellín-Yarumal and Santa Marta areas, Colombia and their Rb/Sr ages. *Journal of the Geological Society of Japan* 82 (9): 559-563.
- González, H. 1980. Geología de la planchas 167 (Sonsón) y 187 (Salamina) escala 1: 100.000. Boletín Geológico INGEOMINAS 23 (1): 1-174.
- Ibáñez-Mejía, M.; Tassinari, C.C.G.; Jaramillo, J.M. 2007. U-Pb zircon ages of the "Antioquian Batholith": Geochronological constraints of late Cretaceous magmatism in the central Andes of Colombia. In *Congreso Colombiano de Geología*, No. 11. Abstract: 11 p. Paipa.
- Jaramillo, J.S.; Cardona, A.; Leon, S.; Valencia, V.; Vinasco, C. 2017. Geochemistry and geochronology from Cretaceous magmatic and sedimentary rocks at 6350 N, western flank of the Central cordillera (Colombian Andes): Magmatic record of arc growth and collision. *Journal of South American Earth Sciences* 76: 460-481.
- Kerr, A.C.; Tarney, J.; Marriner, G.F.; Nivia, A.; Saunders, A.D. 1997. The Caribbean-Colombian Cretaceous igneous province: the internal anatomy of an oceanic plateau. Large igneous provinces: Continental, oceanic, and planetary flood volcanism: 123-144.
- Leal-Mejía, H. 2011. Phanerozoic Gold Metallogeny in the Colombian Andes: A Tectono-magmatic Approach: Ph.D. thesis (Unpublished), Universitat de Barcelona: 1000 p.
- Lozano-Santa Cruz, R.; Verma, S.P.; Girón, P.; Velasco, F.; Morán, D.; Viera, F.; Chávez, G. 1995. Calibración preliminar de fluorescencia de rayos X para análisis cuantitativo de elementos mayores en rocas ígneas. *Actas Instituto Nacional de Geoquímica* 1: 203-208.
- Ludwig, K.R. 2004. Isoplot/Ex: a geochronological toolkit for Microsoft Excel. Version 3. Berkeley, Berkeley Geochronology Center Publ. 4.
- Martens, U.; Restrepo, J.J.; Ordóñez-Carmona, O.; Correa-Martínez, A.M. 2014. The Tahamí and Anaconda terranes of the Colombian Andes: missing links between the South American and Mexican Gondwana margins. *The Journal of Geology* 122 (5): 507-530.
- Middlemost, E. A. 1994. Naming materials in the magma/igneous rock system. *Earth-Science Reviews* 37 (3-4): 215-224.
- Montes, C.; Guzmán, G.; Bayona, G.; Cardona, A.; Valencia, V.; Jaramillo, C. 2010. Clockwise rotation of the Santa Marta massif and simultaneous Paleogene to Neogene deformation of the Plato-San Jorge and Cesar-Ranchería basins. *Journal of South American Earth Sciences* 29 (4): 832-848.

- Mora-Bohórquez, J.A.; Ibáñez-Mejía, M.; Oncken, O.; de Freitas, M.; Vélez, V.; Mesa, A.; Serna, L. 2017. Structure and age of the Lower Magdalena Valley basin basement, northern Colombia: New reflection-seismic and U-Pb-Hf insights into the termination of the central andes against the Caribbean basin. *Journal of South American Earth Sciences* 74: 1-26.
- Mori, L.; Gómez-Tuena, A.; Schaaf, P.; Goldstein, S.L.; Pérez-Arvizu, O.; Solís-Pichardo, G. 2009. Lithospheric removal as a trigger for flood basalt magmatism in the Trans-Mexican Volcanic Belt. *Journal of Petrology* 50 (11): 2157-2186. doi: 10.1093/petrology/egp072.
- Ordóñez-Carmona, O. 1997. O Pré-cambriano na parte norte da Cordilheira Central dos Andes colombianos. Tesis de maestría (Inédito), Universidad de Brasilia: 90 p.
- Ordóñez-Carmona, O.; Pimentel, M. 2001. Consideraciones geocronológicas e isotópicas del Batolito Antioqueño. *Revista de la Academia colombiana de ciencias exactas, físicas y naturales* 25 (94-97): 27 p.
- Ordóñez-Carmona, O.; Álvarez, J.J.R.; Pimentel, M.M. 2006. Geochronological and isotopical review of pre-Devonian crustal basement of the Colombian Andes. *Journal of South American Earth Sciences* 21 (4): 372-382.
- Paton, C.; Woodhead, J.D.; Hellstrom, J.C.; Hergt, J.M.; Greig, A.; Maas, R. 2010. Improved laser ablation U-Pb zircon geochronology through robust downhole fractionation correction. *Geochemistry, Geophysics, Geosystems* 11 (3): Q0AA06. doi: 10.1029/2009GC002618.
- Peccerillo, A.; Taylor, S.R. 1976. Geochemistry of Eocene calc-alkaline volcanic rocks from the Kastamonu area, northern Turkey. Contributions to mineralogy and petrology 58 (1): 63-81.
- Pérez, G. 1967. Determinación de la edad de algunas rocas ígneas de Antioquia por el método K-Ar. Tesis de pregrado (Inédito), Universidad Nacional de Colombia: 46 p.
- Pindell, J.L.; Kennan, L. 2009. Tectonic evolution of the Gulf of Mexico, Caribbean and northern South America in the mantle reference frame: an update. *Geological Society, Special Publications* 328 (1): 1-55. London.
- Pindell, J.L.; Higgs, R.; Dewey, J.F. 1998. Cenozoic palinspastic reconstruction, paleogeographic evolution, and hydrocarbon setting of the northern margin of South America. In *Paleogeographic Evolution and Non-Glacial Eustasy, Northern South America: SEPM* (Pindell, J.L., Drake, C.L.; editors), Special Publication 58: 45-86.
- Pindell, J.; Kennan, L.; Maresch, W.V.; Stanek, K.P.; Draper, G.; Higgs, R. 2005. Plate-kinematics and crustal dynamics of circum-Caribbean arc-continent interactions: Tectonic controls on basin development in Proto-Caribbean margins. *Geological Society of America Special Papers* 394: 7-52.
- Pindell, J.L.; Kennan, L.; Stanek, K.P.; Maresch, W.V.; Draper, G.G. 2006. Foundations of Gulf of Mexico and Caribbean evolution: eight controversies resolved. *Acta Geologica* 4: 303-341.
- Ramos, V.A. 2009. Anatomy and global context of the Andes: Main geologic features and the Andean orogenic cycle. *Geological Society of America Memoirs* 204: 31-65.
- Ramos, V.A.; Aleman, A. 2000. Tectonic evolution of the Andes. *Tectonic Evolution of South America* 31: 635-685.
- Restrepo-Moreno, S.A.; Foster, D.A.; Kamenov, G.D. 2007. Formation age and magma sources for the Antioqueño and Ovejas batholiths derived from U-Pb dating and Hf isotope analysis of zircon grains. *Geological Society of America Progr* 39 (6).
- Restrepo-Moreno, S.A.; Foster, D.A.; Stockli, D.F.; Parra-Sánchez, L.N. 2009. Long-term erosion and exhumation of the “Altiplano Antioqueño”, Northern Andes (Colombia) from apatite (U-Th)/He thermochronology. *Earth and Planetary Science Letters* 278 (1): 1-12.
- Restrepo, J.J.; Ibáñez-Mejía, M.; García-Casco, A. 2012. U-Pb zircon ages of the Medellin Amphibolites (Central Cordillera of Colombia) reveal mid-Cretaceous tectonic juxtaposition of Triassic and mid-Cretaceous metamorphic complexes. In *Simposio Sudamericano de Geología Isotópica*, No. 8, Medellín.
- Restrepo, J.J. 1991. Datación de algunas cenizas volcánicas de Antioquia por el método de trazas de fisión. In *Environmental Geology and Applied Geomorphology in Colombia* (López Rendón, J.E.; editors). Universidad EAFIT, Association of Geoscientists for International Development Report 16: 148-1.
- Restrepo, J.J.; Toussaint, J.F. 1990. Cenozoic arc magmatism of northwestern Colombia. *Geological Society of America Special Papers* 241: 205-212.
- Sáenz, C.T.; Hackspacher, P.C.; Neto, J.H.; Iunes, P.J.; Guedes, S.; Ribeiro, L.F.B.; Paulo, S.R. 2003. Recognition of Cretaceous, Paleocene, and Neogene tectonic reactivation through apatite fission-track analysis in Precambrian areas of southeast Brazil: association with the opening of the South Atlantic Ocean. *Journal of South American Earth Sciences* 15 (7): 765-774.
- Sáenz, E.A.; Paucar, C.G.; Restrepo, J.J. 1996. Estudio de la evolución térmica del Batolito Antioqueño por

- huellas de fisión. *In Congreso Colombiano de Geología, No. 7, Memorias 2:* 240-251. Bogotá.
- Salazar, C.A.; Bustamante, C.; Archango, C.J. 2016. Magnetic fabric (AMS, AAR) of the Santa Marta batholith (northern Colombia) and the shear deformation along the Caribbean Plate margin. *Journal of South American Earth Sciences* 70: 55-68.
- Sarmiento-Rojas, L.F.; Van Wess, J.D.; Cloetingh, S. 2006. Mesozoic transtensional basin history of the Eastern Cordillera, Colombian Andes: Inferences from tectonic models. *Journal of South American Earth Sciences* 21 (4): 383-411.
- Shand, S.J. 1943. Eruptive rocks: their genesis, composition, classification, and their relation to ore deposits with a chapter on meteorites 552 (1): S43.
- Sláma, J.; Košler, J.; Condon, D.J.; Crowley, J.L.; Gerdes, A.; Hanchar, J.M.; Horstwood, M.S.; Morris, G.A.; Nasdala, L.; Norberg, N.; Schaltegger, U. 2008. Plešovice zircon-a new natural reference material for U-Pb and Hf isotopic microanalysis. *Chemical Geology* 249 (1): 1-35.
- Solari, L.A.; Tanner, M. 2011. UPb. age, a fast data reduction script for LA-ICP-MS U-Pb geochronology. *Revista Mexicana de Ciencias Geológicas* 28 (1).
- Solari, L.A.; Gómez-Tuena, A.; Bernal, J.P.; Pérez-Arvizu, O.; Tanner, M. 2010. U-Pb Zircon Geochronology with an Integrated LA-ICP-MS Microanalytical Workstation: Achievements in Precision and Accuracy. *Geostandards and Geoanalytical Research* 34 (1): 5-18.
- Spikings, R.A.; Winkler, W.; Hughes, R.A.; Handler, R. 2005. Thermochronology of allochthonous terranes in Ecuador: Unravelling the accretionary and post-accretionary history of the Northern Andes. *Tectonophysics* 399 (1): 195-220.
- Spikings, R.; Cochrane, R.; Villagómez, D.; Van der Lelij, R.; Vallejo, C.; Winkler, W.; Beate, B. 2015. The geological history of northwestern South America: From Pangaea to the early collision of the Caribbean large igneous province (290-75 Ma). *Gondwana Research* 27 (1): 95-139.
- Toro, G.E.; Hermelin, M.; Schwabe, E.; Posada, B.; Silva, D.; Poupeau, G. 2006. Fission-track datings and geomorphic evidences for long-term stability in the Central Cordillera highlands, Colombia. *Zeitschrift für Geomorphologie, Supplementbände* 145: 1-16.
- Vallejo, C.; Winkler, W.; Spikings, R.A.; Luzieux, L.; Heller, F.; Bussy, F. 2009. Mode and timing of terrane accretion in the forearc of the Andes in Ecuador. *Geological Society of America Memoirs* 204: 197-216.
- Villagómez, D. 2010. Thermochronology, geochronology and geochemistry of the Western and Central cordilleras and Sierra Nevada de Santa Marta, Colombia: The tectonic evolution of NW South America. Tesis de doctorado, Universidad de Ginebra: 143 p. Ginebra.
- Villagómez, D.; Spikings, R. 2013. Thermochronology and tectonics of the Central and Western cordilleras of Colombia: Early Cretaceous-Tertiary evolution of the northern Andes. *Lithos* 160-161: 228-249.
- Villagómez, D.; Spikings, R.; Magna, T.; Kammer, A.; Winkler, W.; Beltrán, A. 2011. Geochronology, geochemistry and tectonic evolution of the Western and Central cordilleras of Colombia. *Lithos* 125 (3-4): 875-896.
- Villamil, T. 1999. Campanian-Miocene tectonostratigraphy, depocenter evolution and basin development of Colombia and western Venezuela. *Palaeogeography, Palaeoclimatology, Palaeoecology* 153 (1): 239-275.
- Whattam, S.A.; Stern, R.J. 2015. Late Cretaceous plume-induced subduction initiation along the southern margin of the Caribbean and NW South America: The first documented example with implications for the onset of plate tectonics. *Gondwana Research* 27 (1): 38-63.
- Wood, D.A. 1979. A variably veined suboceanic upper mantle-genetic significance for mid-ocean ridge basalts from geochemical evidence. *Geology* 7 (10): 499-503.
- Wright, J.E.; Wyld, S.J. 2011. Late Cretaceous subduction initiation on the eastern margin of the Caribbean-Colombian Oceanic Plateau: One Great Arc of the Caribbean (?). *Geosphere* 7 (2): 468-493.
- Zapata, J.; Correa, T.; Obando, M.; Rincón, A.; Ortiz, F.; Rodríguez, G. 2017. Redefinición cronoestratigráfica del Batolito de Sabanalarga. *In Congreso Colombiano de Geología, No. 16 y Simposio de Exploradores, No. 3, Memorias:* 1472-1477